Nonlinear Analysis: Modelling and Control, 2004, Vol. 9, No. 3, 203–218

Computational Modelling of a Sensor Based on an Array of Enzyme Microreactors *

R. Baronas[1], F. Ivanauskas[1,2], J. Kulys[3], M. Sapagovas[2]

[1]Vilnius University, Naugarduko st. 24, 03225 Vilnius, Lithuania
romas.baronas@maf.vu.lt

[2]Institute of Mathematics and Informatics, Akademijos st. 4, 08663 Vilnius, Lithuania
feliksas.ivanauskas@maf.vu.lt

[3]Vilnius Gediminas Technical University, Saulėtekio av. 11, 11223 Vilnius, Lithuania
juozas.kulys@fm.vtu.lt

Received: 17.05.2004
Accepted: 09.06.2004

Abstract. This paper presents a two-dimensional-in-space mathematical model of a sensor system based an array of enzyme microreactors immobilised on a single electrode. The system acts under amperometric conditions. The model is based on the diffusion equations containing a non-linear term related to the Michaelis-Menten kinetics of the enzymatic reaction. The model involves three regions: an array of enzyme microreactors (cells) where enzyme reaction as well as mass transport by diffusion takes place, a diffusion limiting region where only the diffusion takes place, and a convective region, where the analyte concentration is maintained constant. Using computer simulation the influence of the geometry of the enzyme cells and the diffusion region on the biosensor response was investigated. The digital simulation was carried out using the finite difference technique.

Keywords: reaction-diffusion, modelling, biosensor, microreactor.

1 Introduction

A sensor is a device that converts a physical or chemical quantity to an electrical one [1]. The term biosensor refers to sensors that use biological components,

*This work was supported by Lithuanian State Science and Studies Foundation, project No. C-03048.

usually enzymes, which catalyse the interaction with analyte [2]–[4].The amperometric biosensors measure the faradaic current that arises on a working indicator electrode by direct electrochemical oxidation or reduction of the products of the biochemical reaction [5, 6]. In amperometric biosensors the potential at the electrode is held constant while the current is measured. The amperometric biosensors are known to be reliable, cheap and highly sensitive for environment, clinical and industrial purposes [7, 8].

In some applications of biosensors, enzymes are archival and only available in every limited quantity or are the products of commbinatorial synthesis procedures and thus are only produced in microgram to milligram quantities. These include point-of-care testing [9], high throughput drug discovery [10], detection of biological warfare agents [11], astrobiology [12] and others. Such applications of biosensors requires high-density arrays of microvolume reaction vessels. Because of this, miniaturization of biosensors is very important trend in biotechnology. The application of arrays of microreactors is one way of the miniaturization.

Since it is not generally possible to measure the concentration of substrate inside enzyme domain with analytical devices, starting from seventies various mathematical models of amperometric biosensors have been developed and used as an important tool to study and optimise analytical characteristics of actual biosensors [13]–[16].The goal of this investigation is to make a model allowing an effective computer simulation of a sensor system based an array of enzyme cells (microreactors) immobilised on a single electrode.

The developed model is based on diffusion equations [17, 18], containing a non-linear term related to the Michaelis-Menten kinetics of the enzymatic reaction. The model involves three regions: an array of enzyme cells where enzyme reaction as well as mass transport by diffusion takes place, a diffusion limiting region where only the diffusion takes place, and a convective region, where the analyte concentration is maintained constant. The enzyme domain was modelled by identical right cylinders, arranged in a rigid hexagonal array and distributed uniformly on the electrode surface. Using computer simulation the influence of the geometry of the enzyme cells as well as the diffusion region on the biosensor response was investigated. The computer simulation was carried out using the finite difference technique [19].

2 Principal structure of a biosensor system

Fig. 1 shows a biosensor system, where the enzyme microreactors are modelled by identical cylinders of radius a and height c. The enzyme cylinders are arranged in a rigid hexagonal array. The distance between centres of two adjacent cylinders equals $2b$.

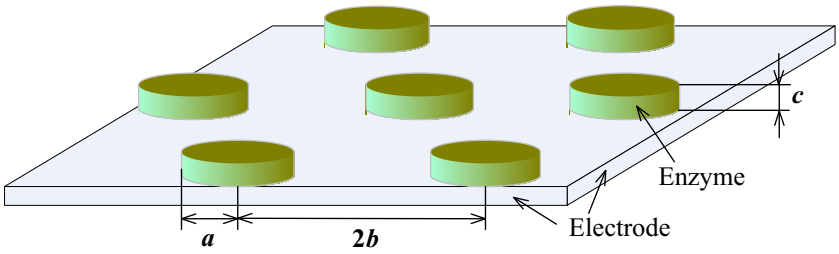

Fig. 1. A principal structure of an array of enzyme microreactors immobilised on a single electrode. The figure is not to scale.

We assume that the mass transport during the biosensor action obeys a finite diffusion regime. A principal structure of the electrode and the profile of the biosensor at z plane are depicted in Fig. 2.

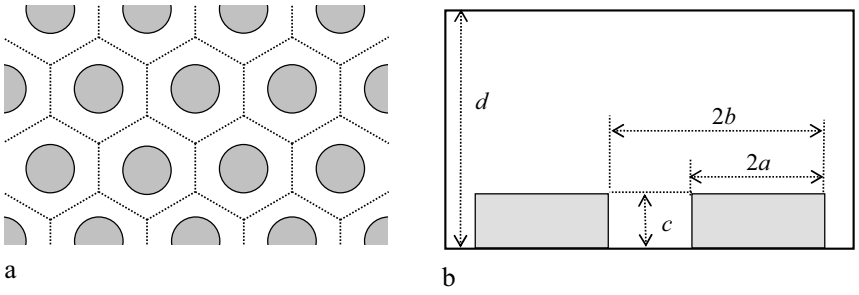

Fig. 2. A principal structure of the enzyme electrode (a) and the profile at z plane (b). d is the thickness of the diffusion layer.

Assuming the uniform distribution of the enzyme microreactors on the electrode surface, the biosensor may be divided into equal hexagonal prisms with

regular hexagonal bases. For simplicity, it is reasonable to consider a circle of radius b whose area equals to that of the hexagon and to regard one of the cylinders as a unit cell. Due to the symmetry of the unit cell, we may consider only a half of the transverse section of the unit cell. Very similar approach has been used in modelling of partially blocked electrodes [20, 21] and in modelling of surface roughtness of the enzyme membrane [22].

3 Mathematical model

A biosensor may be considered as an electrode, having a layer of enzyme applied onto the electrode surface. We consider a scheme of catalysed with enzyme (E) substrate (S) conversion to the product (P) [4]

$$\mathrm{S} \xrightarrow{\mathrm{E}} \mathrm{P} \tag{1}$$

Fig. 3 shows the considered domain of the unit of the biosensor, presented schematically in Figs. 1 and 2. In the profile, parameter b stands for the radius of the entire cell, while a stands for the radius of the enzyme microreactor. c is the height of the enzyme microreactor. The fourth parameter d is the thickness of the diffusion layer.

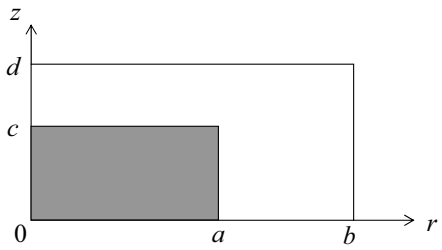

Fig. 3. The considered domain of the biosensor unit.

The diffusion region surrounding the enzyme cells is known as the Nernst diffusion layer [23]. According to the Nernst approach, the diffusion takes place in a finite layer of the buffer solution. Away from it, the solution is in motion and uniform in concentration. The thickness of the Nernst layer remains unchanged with time. If substrate is well-stirred and in powerful motion, then rather often

the Nernst diffusion layer is neglected [14, 24]. However, in practice, the zero thickness of the Nernst layer can not be achieved [6, 23]. Because of this, we assume that the mass transport during the biosensor action obeys a finite diffusion regime.

Let Ω, Ω_0 be open regions corresponding to the entire domain to be considered and enzyme region, respectively, and Γ - the bulk solution/enzyme border.

$$\begin{aligned}
\Omega &= \big\{(r,z)\colon 0<r<b,\ 0<z<d\big\},\\
\Omega_0 &= \big\{(r,z)\colon 0<r<a,\ 0<z<c\big\},\\
\Gamma &= \big\{(a,z)\colon 0\le z\le c\big\}\cup\big\{(r,c)\colon 0\le r\le a\big\}.
\end{aligned} \tag{2}$$

Let $\overline{\Omega}$ and $\overline{\Omega}_0$ denote the corresponding closed regions. The dynamics of the biosensor is described by the reaction-diffusion system ($t>0$)

$$\begin{aligned}
\frac{\partial S_e}{\partial t} &= D_{S_e}\frac{1}{r}\frac{\partial}{\partial r}\left(r\frac{\partial S_e}{\partial r}\right)+D_{S_e}\frac{\partial^2 S_e}{\partial z^2}-\frac{V_{max}S_e}{K_M+S_e},\\
\frac{\partial P_e}{\partial t} &= D_{P_e}\frac{1}{r}\frac{\partial}{\partial r}\left(r\frac{\partial P_e}{\partial r}\right)+D_{P_e}\frac{\partial^2 P_e}{\partial z^2}+\frac{V_{max}S_e}{K_M+S_e},\quad (r,z)\in\Omega_0,
\end{aligned} \tag{3}$$

$$\begin{aligned}
\frac{\partial S_b}{\partial t} &= D_{S_b}\frac{1}{r}\frac{\partial}{\partial r}\left(r\frac{\partial S_b}{\partial r}\right)+D_{S_b}\frac{\partial^2 S_b}{\partial z^2},\\
\frac{\partial P_b}{\partial t} &= D_{P_b}\frac{1}{r}\frac{\partial}{\partial r}\left(r\frac{\partial P_b}{\partial r}\right)+D_{P_b}\frac{\partial^2 P_b}{\partial z^2},\quad (r,z)\in\Omega\setminus\overline{\Omega}_0,
\end{aligned} \tag{4}$$

where r and z stand for space, t stands for time, $S_e(r,z,t)$, $S_b(r,z,t)$ ($P_e(r,z,t)$, $P_b(r,z,t)$) are the substrate (reaction product) concentrations in the enzyme and bulk solution, respectively, D_{S_e}, D_{S_b}, D_{P_e}, D_{P_b} are the diffusion coefficients, V_{max} is the maximal enzymatic rate and K_M is the Michaelis constant.

In the domain presented in Fig. 3, $z=0$ represents the electrode surface, and Γ corresponds to the bulk solution/enzyme interface. The biosensor operation starts when the substrate appears over the surface of the enzyme region. This is used in the initial conditions ($t=0$)

$$\begin{aligned}
&S_e(r,z,0)=0, \quad P_e(r,z,0)=0, \quad (r,z)\in\overline{\Omega}_0\setminus\Gamma,\\
&S_e(r,z,0)=S_0, \quad P_e(r,z,0)=0, \quad (r,z)\in\Gamma,\\
&S_b(r,z,0)=S_0, \quad P_b(r,z,0)=0, \quad (r,z)\in\overline{\Omega}\setminus\Omega_0,
\end{aligned} \tag{5}$$

where S_0 is the concentration of the substrate to be analyzed.

The following boundary conditions express the symmetry of the biosensor

$$\begin{aligned}
&\left.\frac{\partial S_e}{\partial r}\right|_{r=0} = \left.\frac{\partial P_e}{\partial r}\right|_{r=0} = 0, \quad z \in [0, c],\\
&\left.\frac{\partial S_b}{\partial r}\right|_{r=0} = \left.\frac{\partial P_b}{\partial r}\right|_{r=0} = 0, \quad z \in [c, d],\\
&\left.\frac{\partial S_b}{\partial r}\right|_{r=b} = \left.\frac{\partial P_b}{\partial r}\right|_{r=b} = 0, \quad z \in [0, d].
\end{aligned} \tag{6}$$

In the scheme (1) the product (P) is electro-active substance. The electrode potential is chosen to keep zero concentration of the product at the electrode surface. The substrate (S) does not react at the electrode surface. This is used in the boundary conditions ($t > 0$) given by

$$\begin{aligned}
&P_e(r, 0, t) = 0, \quad \left.\frac{\partial S_e}{\partial z}\right|_{z=0} = 0, \qquad r \in [0, a],\\
&P_b(r, 0, t) = 0, \quad \left.\frac{\partial S_b}{\partial z}\right|_{z=0} = 0, \qquad r \in [a, b],\\
&P_b(r, d, t) = 0, \quad S_b(r, d, t) = S_0, \qquad r \in [0, b].
\end{aligned} \tag{7}$$

On the surface Γ we define the matching conditions ($t > 0$)

$$\begin{aligned}
&D_{S_e}\left.\frac{\partial S_e}{\partial \mathrm{n}}\right|_{\Gamma} = D_{S_b}\left.\frac{\partial S_b}{\partial \mathrm{n}}\right|_{\Gamma}, \quad S_e\big|_{\Gamma} = S_b\big|_{\Gamma},\\
&D_{P_e}\left.\frac{\partial P_e}{\partial \mathrm{n}}\right|_{\Gamma} = D_{P_b}\left.\frac{\partial P_b}{\partial \mathrm{n}}\right|_{\Gamma}, \quad P_e\big|_{\Gamma} = P_b\big|_{\Gamma},
\end{aligned} \tag{8}$$

where n stands for the normal direction.

We introduce the concentration S of the substrate S and the concentration P of the reaction product P in entire domain $\overline{\Omega}$ as follows ($t \geq 0$):

$$\begin{aligned}
S(r, z, t) &= \begin{cases} S_e(r, z, t), & (r, z) \in \overline{\Omega}_0,\\ S_b(r, z, t), & (r, z) \in \overline{\Omega} \setminus \overline{\Omega}_0, \end{cases}\\
P(r, z, t) &= \begin{cases} P_e(r, z, t), & (r, z) \in \overline{\Omega}_0,\\ P_b(r, z, t), & (r, z) \in \overline{\Omega} \setminus \overline{\Omega}_0. \end{cases}
\end{aligned} \tag{9}$$

Both concentration functions: S and P are continuous in the entire domain $(r, z) \in \overline{\Omega}$, $t \geq 0$.

In a special case when $a = b$, the model (3)–(8) describes an operation of the membrane biosensors [3, 4, 25].

The measured current is accepted as a response of a biosensor in a physical experiment. The current depends upon the flux of the electro-active substance (product) at the electrode surface, i.e. on the border $z = 0$. Consequently, a density $i(t)$ of the biosensor current at time t can be obtained explicitly from the Faraday's and Fick's laws

$$\begin{aligned} i(t) &= \frac{n_e F}{\pi b^2} \int_0^{2\pi} \left(\int_0^a D_{P_e} \frac{\partial P_e}{\partial z}\bigg|_{z=0} r dr + \int_a^b D_{P_b} \frac{\partial P_b}{\partial z}\bigg|_{z=0} r dr \right) d\varphi = \\ &= \frac{2 n_e F}{b^2} \left(D_{P_e} \int_0^a \frac{\partial P_e}{\partial z}\bigg|_{z=0} r dr + D_{P_b} \int_a^b \frac{\partial P_b}{\partial z}\bigg|_{z=0} r dr \right), \end{aligned} \tag{10}$$

where φ is the third cylindrical coordinate, n_e is a number of electrons involved in a charge transfer, F is the Faraday constant, $F = 9648\,\mathrm{C/mol}$.

We assume, that the system (3)–(8) approaches a steady-state as $t \to \infty$

$$i_\infty = \lim_{t \to \infty} i(t). \tag{11}$$

i_∞ is assumed as the steady-state biosensor current.

4 Computer simulation

Close mathematical solutions are not usually possible when analytically solving multi-dimensional non-linear partial differential equations with complex boundary conditions. Therefore, the problem was solved numerically [17, 24].

The finite difference technique was applied for discretization of the mathematical model [19]. We introduced an uniform discrete grid in all directions: r, z and t [22, 25]. Using the alternating direction method, an implicit finite difference scheme has been built as a result of the difference approximation of the model. The resulting systems of linear algebraic equations were solved efficiently because of the tridiagonality of their matrices. Having a numerical solution of the problem, the density of the biosensor current was calculated easily. The software was programmed in Fortran language [26].

The mathematical model as well as the numerical solution of the model were evaluated for different values of the maximal enzymatic rate V_{max}, substrate concentration S_0 and the geometry of the enzyme microreactors.

We assumed the upper layer of the thickness $\delta_N = d - c$ from the enzyme region as the Nernst diffusion layer. The thickness δ_N of the Nernst layer depends upon the nature and stirring of the buffer solution. Usually, the more intensive stirring corresponds to the thinner diffusion layer. In practice, the zero thickness of the Nernst layer can not be achieved. In a case when the solution to be analysed is stirred by rotation of the enzyme electrode, the thickness δ_N of the Nernst diffusion layer may be minimized up to 0.02 mm by increasing the rotation speed [6, 23]. That thickness of the Nernst layer, $\delta_N = d - c = 0.02$ mm, we used to simulate the biosensor action changing other parameters.

The following values of the parameters were constant in the numerical simulation of all the experiments:

$$\begin{aligned} &D_{S_e} = D_{P_e} = 3.0 \times 10^{-10}\,\mathrm{m}^2/\mathrm{s}, \\ &D_{S_b} = 2D_{S_e}, \quad D_{P_b} = 2D_{P_e}, \\ &K_M = 0.1\,\mathrm{mol/m}^3 = 100\,\mu\mathrm{M}, \\ &\delta_N = d - c = 0.02\,\mathrm{mm}, \quad n_e = 2. \end{aligned} \tag{12}$$

The steady-state biosensor current i_∞ (the biosensor response) as well as the time moment of occurrence of the steady-state current (response time) were assumed and analysed as ones of the most important characteristics of biosensors.

In digital simulation, the biosensor response time was assumed as the time when the absolute current slope value falls below a given small value normalised with the current value. In other words, the time

$$t_R = \min_{i(t)>0} \left\{ t\colon \frac{1}{i(t)} \left| \frac{\partial i(t)}{\partial t} \right| < \varepsilon \right\} \tag{13}$$

needed to achieve a given dimensionless decay rate ε was used.

Consequently, the current $i_R = i(t_R)$ at the biosensor response time t_R was assumed as the steady-state biosensor current i_∞, $i_R \approx i_\infty$. In calculations, we used $\varepsilon = 10^{-6}$.

Figs. 4 and 5 show the substrate and product concentrations at steady-state conditions ($t_R = 67$ s) accepting $a = c = 0.1$ mm, $b = 2c = 0.2$ mm, $d = c + \delta_N = 0.12$ mm, $V_{max} = 100\,\mu$M/s, $S_0 = 20\,\mu$M.

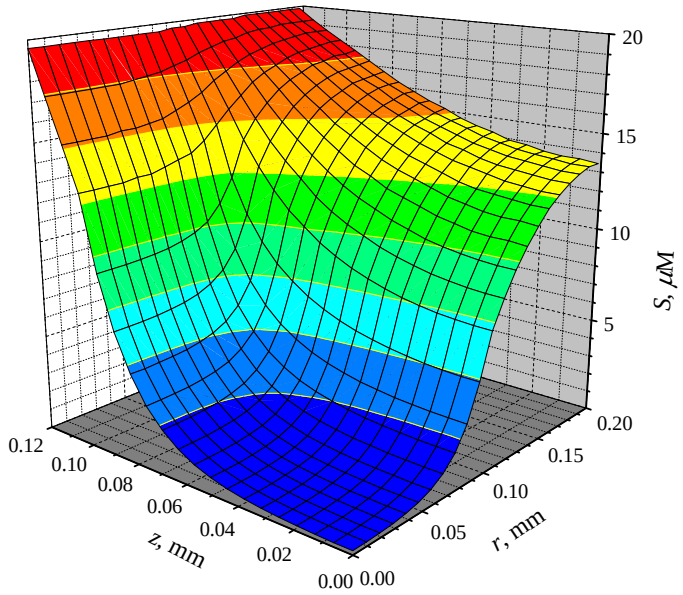

Fig. 4. The concentration S of the substrate at steady-state conditions, $t_R = 67$ s, $a = 0.1$, $b = 0.2$, $c = 0.1$, $d = 0.12$ mm, $V_{max} = 100\mu$M/s, $S_0 = 20\mu$M.

5 Results and discussion

Using numerical simulation, the influence of the geometry of the enzyme microreactors on the steady-state current was investigated.

Firstly, we calculate values i of the the biosensor current at different radiuses of the enzyme reactor keeping all other parameters constant. Fig. 6 shows the dynamics of the biosensor current at six values of the radius a. The parameter a varies from $0.1b$ to b. All other parameters are the same as in Fig. 4.

Fig. 6 shows that the parameter a significantly effects the steady-state current i_R as well as the response time t_R. In the case of the continuous membrane ($a = b$), the biosensor current i is a monotonous increasing function of time t. At all other cases when $a < b$, i is a non-monotonous function of t. However, the maximal relative difference between the maximal current and the steady-state one only reaches about 6% at $a = 0.12$ mm.

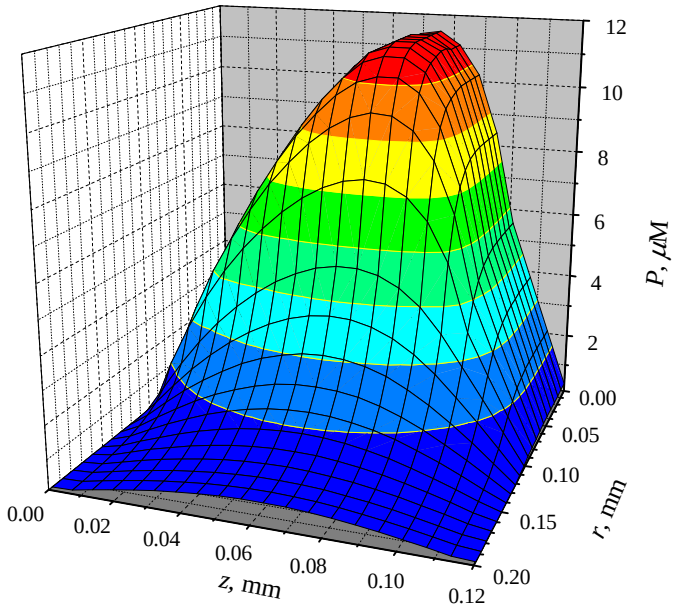

Fig. 5. The concentration P of the reaction product. All the parameters are the same as in Fig. 4.

One can see in Fig. 6, that the maximal and steady-state currents are non-monotonous functions of the radius a of the enzyme cell. To investigate that effect in details we calculate the steady-state current i_R at different values of the radius b of entire cell changing the radius a with a small step.

Fig. 7 shows the steady-state current i_R versus the ratio $k = a/b$ at four values of the radius b: $0.1,\ 0.2,\ 0.4$ and $0.8\,$mm. Fig. 7 shows that i_R is a non-monotonous function of the ratio k at all values of b. In the case of $b = 0.1\,$mm, the relative difference between i_R at $k = 0.7$ and another one at $k = 1$ exceeds 13%. The case when $k = 1$ corresponds to a membrane biosensor. Since the height c of enzyme reactor was the same in all the calculations, then the volume of enzyme microreactor is directly proportional to ratio k. Although, the biosensor, based on an array of microreactors, is of less enzyme volume than the corresponding membrane one, the array biosensor can generate even higher steady-state current

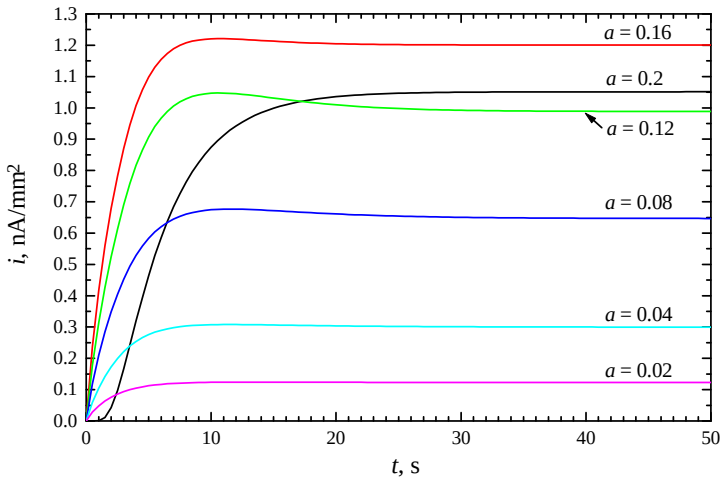

Fig. 6. The dynamics of the biosensor current i at different values of the radius a (mm) of the enzyme cell, other parameters are the same as in Fig. 4.

than the membrane one.

The biosensor response considerably depends on the fact either enzyme kinetics or the mass transport predominate in the biosensor response [3, 4, 27]. The biosensor response is known to be under mass transport control if the enzymatic reaction in the enzyme layer is faster than the transport process. In the case of the membrane biosensors ($a = b$), the diffusion modulus (Damköhler number) σ^2 essentially compares the rate of enzyme reaction (V_{max}/K_M) with the diffusion through the enzyme layer (D_{S_e}/c^2) [13, 18]

$$\sigma^2 = \frac{V_{max}c^2}{D_{S_e}K_M}, \tag{14}$$

where c is assumed as the thickness of the enzyme membrane. If $\sigma^2 < 1$, the enzyme kinetics controls the biosensor response. The response is under diffusion control when $\sigma^2 > 1$. The model (3)–(8) applies to the enzyme membrane biosensors when $a = b$ is assumed.

At values of D_{S_e} and K_M given in (12), $c = 0.1$ mm, and $V_{max} = 100\mu$M/s the diffusion modulus σ^2 equals approximately 33.3. Consequently, Figs. 4–7 show the biosensor behaviour in the case when the response is under diffusion

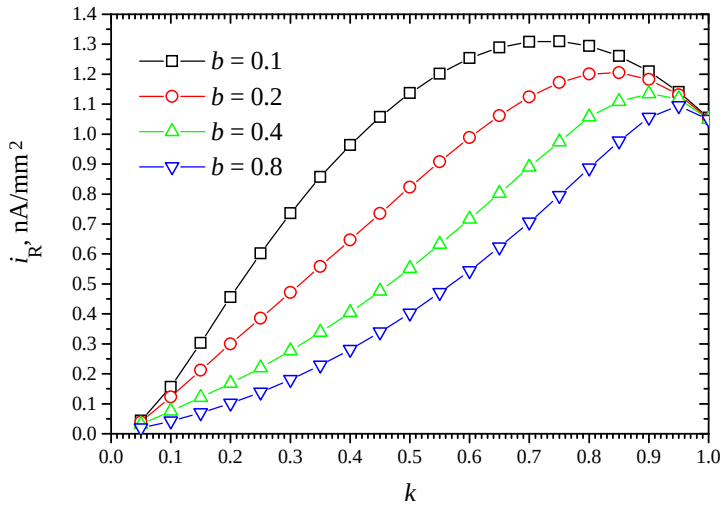

Fig. 7. The steady-state current i_R versus the ratio $k = a/b$ at four values of the radius b: $0.1,\ 0.2,\ 0.4$ and 0.8 mm, other parameters are the same as in Fig. 4.

control.

To investigate the dynamics of the current in the case when the enzyme kinetics controls the biosensor response, we calculate the biosensor current at 10 times thinner enzyme cells, $c = 0.01$ mm, keeping other parameters unchanged. In the case of $c = 0.01$ mm, the diffusion modulus σ^2 equals approximately 0.33. Results of calculations are presented in Fig. 8. One can see in Fig. 8, that the steady-state current i_R increases with increase of the ratio k at all values of the radius b.

The steady-state biosensor current is very sensitive to changes of the maximal enzymatic rate V_{max} and substrate concentration S_0 [3, 4, 25, 27]. Changing values of these two parameters, the steady-state current varies even in orders of magnitude. Because of this, we investigate the influence of the geometry of the biosensor cell on the biosensor response at different values of V_{max} and S_0. Due to the sensitivity of the biosensor response to changes of V_{max} and S_0, we normalise the steady-state biosensor current to evaluate the effect of the geometry of the cell on the biosensor response. Let $i_R(k)$ be the steady-state current of an array biosensor at $k = a/b$. Thus $i_R(1)$ corresponds to the steady-state current of a

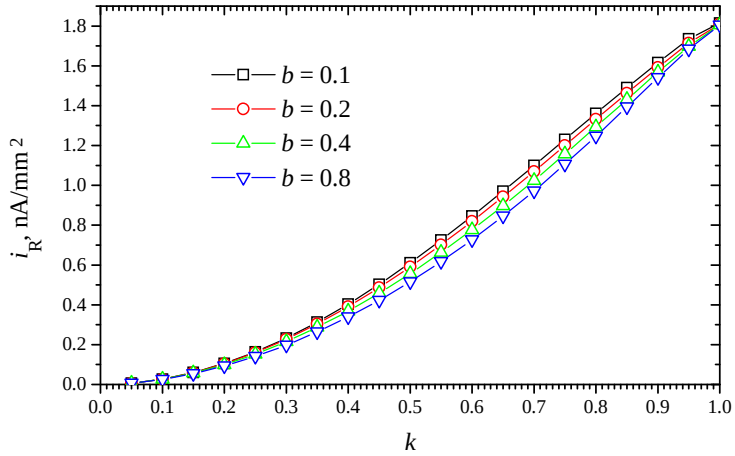

Fig. 8. The steady-state current i_R versus the ratio k at the thickness $d = 0.03$ mm of the diffusion layer, other parameters and notation are the same as in Fig. 7.

membrane biosensor ($a = b$). We express the dimensionless normalised steady-state biosensor current i_{RN} as the steady-state current of the array biosensor ($a < b,\ k < 1$) divided by the steady-state current of the corresponding membrane biosensor ($a = b,\ k = 1$)

$$i_{RN}(k) = \frac{i_R(k)}{i_R(1)}, \quad k = a/b, \quad 0 < k \leq 1. \tag{15}$$

Fig. 9 shows the normalised steady-state current i_{RN} versus the ratio k at two maximal enzymatic rates V_{max}: $10,\ 100\,\mu$M/s and three substrate concentrations S_0: $1,\ 10,\ 100\,\mu$M. In these calculations all other parameters are the same as in Fig. 4. One can see in Fig. 9, i_{RN} is a non-monotonous function of k at $V_{max} = 100\,\mu$M/s while it is a monotonous function at $V_{max} = 10\,\mu$M/s. The diffusion modulus σ^2 equals approximately 33.3 at $V_{max} = 100$ and $\sigma^2 \approx 3.33$ at $V_{max} = 10\,\mu$M/s. Consequentially, the steady-state current is the non-monotonous function of k only in the cases when the biosensor response is significantly under diffusion control $\sigma^2 \gg 1$. The substrate concentration effects the normalised biosensor response slightly only.

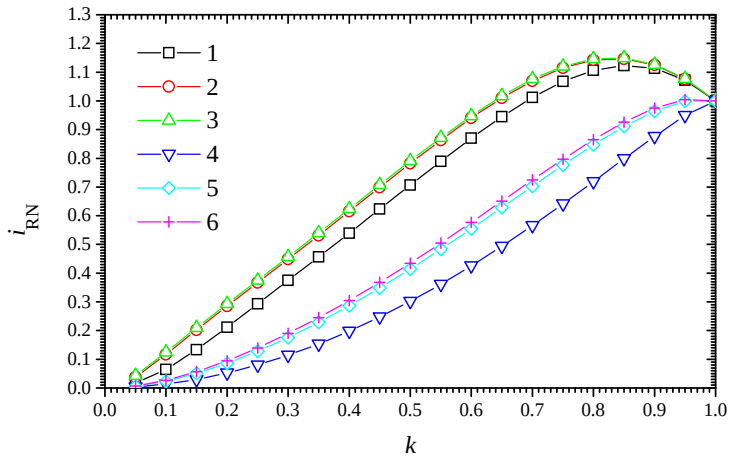

Fig. 9. The normalised steady-state current i_{RN} versus the ratio $k = a/b$ at different enzymatic rates V_{max}: 100 (1-3), 10 (4-6) μM/s and substrate concentration S_0: 100 (3,6), 10 (2, 5), 1 (1, 4) μM, other parameters are the same as in Fig. 4.

6 Conclusions

The mathematical model (3)–(8) can be successfully used to investigate regularities of the response of biosensors based on an array of enzyme microreactors immobilised on a single electrode, where the identical microreactors are arranged in a rigid hexagonal array.

In the cases when the biosensor response is significantly under diffusion control (diffusion modulus $\sigma^2 \gg 1$), the steady-state current is a non-monotonous function of the ratio k of the radius a of the microreactors to the half distance b between centres of two adjacent microreactors (Figs. 7, 9). Otherwise, the steady-state current is a monotonous increasing function of k (Figs. 8, 9).

In the cases when $\sigma^2 \gg 1$, the biosensor, based on an array of microreactors, is able to generate a greater steady-state current than a corresponding membrane biosensor of the enzyme layer thickness being the same as the height of microreactors (Figs. 7, 9). This feature of array biosensors can be applied in design of novel highly sensitive biosensors when the minimization of the enzyme volume is of

crucial importance. Selecting the geometry of microreactors allows to minimize the volume of enzyme without loosing the sensitivity.

References

1. Pallás-Areny R., Webster J. G. *Sensors and Signal Conditioning*, 2nd ed. John Wiley & Sons, New York, 2000
2. Clarc L. C., Loys C. "Electrode system for continuous monitoring in cardiovascular surgery", *Ann. N.Y. Acad. Sci.*, **102**, p. 29–45, 1962
3. Scheller F., Schubert F. *Biosensors*, **7**, Elsevier, Amsterdam, 1988
4. Turner A. P. F., Karube I., Wilson G. S. *Biosensors: Fundamentals and Applications*, Oxford University Press, Oxford, 1987
5. Chaubey A., Malhotra B. D. "Mediated biosensors", *Biosens. Bioelectron.*, **17**, p. 441–456, 2002
6. Kulys J., Razumas V. *Bioamperometry*, Mokslas, Vilnius, 1986 (in Russian)
7. Rogers K. R. "Biosensors for environmental applications", *Biosens. Bioelectron.*, **10**, p. 533–541, 1995
8. Wollenberger U., Lisdat F., Scheller F. W. *Frontiers in Biosensorics 2, Practical Applications*, Birkhauser Verlag, Basel, 1997
9. Dirks J. L. "Diagnostic blood analysis using point-of-care technology", *AACN Clin. Issues*, **7**, p. 249–259, 1996
10. Devlin J. P. (Ed.) *High throughput screening*. Marcel Dekker, New York, 1997
11. Barnaby W. "Biological weapons: an increasing threat", *Med. Confl. Surviv.*, **13**, p. 301–313, 1997
12. Smith J. M., Szathmary E. "On the likelihood of habitable worlds", *Nature*, **384**, p. 107, 1996
13. Kulys J. "The development of new analytical systems based on biocatalysts", *Anal. Lett.*, **14**, p. 377–397, 1981
14. Schulmeister T. "Mathematical treatment of concentration profiles and anodic current of amperometric enzyme electrodes with chemically-amplified response", *Anal. Chim. Acta*, **201**, p. 305–310, 1987
15. Bartlett P. N., Pratt K. F. E. "Modelling of processes in enzyme electrodes", *Biosens. Bioelectron.*, **8**, p. 451–462, 1993

16. Sorochinskii V. V., Kurganov B. I. “Steady-state kinetics of cyclic conversions of substrate in amperometric bienzyme sensors”, *Biosens. Bioelectron.*, **11**, p. 225–238, 1996

17. Crank J. *The Mathematics of Diffusion*, 2nd ed., Clarendon Press, Oxford, 1975

18. Aris R. *The Mathematical Theory of Diffusion and Reaction in Permeable Catalysts. The Theory of the Steady State*, Clarendon Press, Oxford, 1975

19. Ames W. F. *Numerical Methods for Partial Differential Equations*, 2nd ed., Academic Press, New-York, 1977

20. Gueshi T., Tokuda K., Matsuda H. “Voltammetry at partially covered electrodes. Part I. Chronopotentiometry and chronoamperometry at model electrodes”, *J. Electroanal. Chem.*, **89**, p. 247, 1978

21. Deslous C., Gabrielli C., Keddam M., Khalil A., Rosset R., Trobollet B., Zidoune M. “Impedance techniques at partially blocked electrodes by scale deposition”, *Electrochim. Acta*, **42**, p. 1219–1233, 1997

22. Baronas R., Ivanauskas F., Kulys J., Sapagovas M. “Modelling of amperometric biosensors with rough surface of the enzyme membrane”, *J. Math. Chem.*, **34**(3–4), p. 227–242, 2003

23. Wang J. *Analytical Electrochemistry*, 2nd ed. John Wiley & Sons, New-York, 2000

24. Britz D. *Digital Simulation in Electrochemistry*, 2nd ed., Springer-Verlag, Berlin, 1988

25. Baronas R., Ivanauskas F., Kulys J. “Computer simulation of the response of amperometric biosensors in stirred and non stirred solution”, *Nonlinear Analysis: Modelling and Control*, **8**(1), p. 3–18, 2003

26. Press W. H., Flannery B. P., Teukolsky S. A., Vetterling W. T. *Numerical Recipes in Fortran 90: The Art of Scientific Computing*, 2nd ed., Cambridge University Press, Cambridge, 1996

27. Baronas R., Ivanauskas F., Kulys J. “The influence of the enzyme membrane thickness on the response of amperometric biosensors”, *Sensors*, **3**(7), p. 248–262, 2003